ACS OMEGA

http://pubs.acs.org/journal/acsodf

Article

Synergistic Reinforcement of Cellulose Microfibers from Pineapple Leaf and Ionic Cross-Linking on the Properties of Hydrogels

Nithinan Sriraveeroj, Taweechai Amornsakchai,* Panya Sunintaboon, and Anyarat Watthanaphanit

Cite This: *ACS Omega* 2022, 7, 25321−25328

Read Online

ACCESS | Metrics & More | Article Recommendations

ABSTRACT: Hydrogels contain a large amount of water; thus, they are jelly-like, soft, and fragile. Although hydrogels' stiffness and strength can be improved by introducing another network to form a double or interpenetrating network, these mechanical properties are still not enough as many applications demand even stiffer and stronger hydrogels. Different methods of reinforcing hydrogels have been proposed and published. In this research, cellulose microfiber isolated from pineapple leaf was used as the reinforcement for hydrogels. The reinforcing efficiency of the fiber was studied for both single and double networks through the compression test. Other properties such as morphology and swelling behavior of the reinforced hydrogels were also studied. A synergistic effect of the second network and the fiber on the reinforcement was observed. The improvement due to the effect of fiber loading of only 0.6 wt % was found to be as high as 150%. This is greater than that observed in some nanofiller systems. Thus, the fiber can be used as a green reinforcement for similar hydrogel systems.

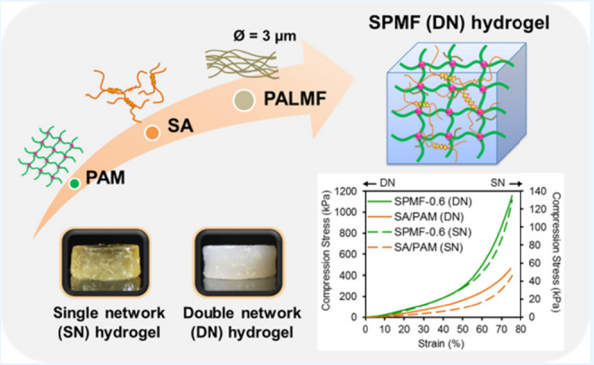

1. INTRODUCTION

Hydrogels are polymer networks containing large amounts of water (~90%).[1,2] They provide many advantages, for example, good biocompatibility, low toxicity, high flexibility similar to that of natural tissue, and low cost. Hydrogels have been widely applied in many fields, including drug delivery, tissue engineering, wastewater treatment, superabsorbent, and so on.[1−4] Nevertheless, some applications might be highly limited due to the poor mechanical properties of hydrogels.[5] Over the past decades, many attempts have been devoted to develop hydrogels with improved mechanical strength, for instance, a topological gel, a tetra-PEG gel, double network (DN) system, and composite hydrogel.[6−13] Among these types, the DN system is very attractive. In 2003, Jian Ping Gong and colleagues proposed the DN hydrogel consisting of two networks as the strongest soft material with a large compressive stress of 17.2 MPa at 92% strain.[8] The improved strength of the hydrogel is ascribed to the different structures of both networks, of which the first one is a densely cross-linked rigid structure and the other is a loosely cross-linked ductile one.[14] During deformation, the rigid network will break into small fragments to dissipate the energy and protect the second network serving as "sacrificial bonds". Until now, the mechanical properties of many hydrogel systems have been improved significantly by exploiting the DN concept.

One of the most DN systems studied is a combination between sodium alginate (SA) and polyacrylamide (PAM). SA is a linear polysaccharide that can be extracted from brown algae. It has received much attention owing to its good biocompatibility and biodegradability.[15,16] PAM is a synthetic polymer which, on the other hand, forms a loose cross-linked structure considered as a good ductile network. PAM also possesses biocompatibility, good flexibility, high stability, and hydrophilicity.[14] It is reported that the SA/PAM DN hydrogel exhibited a higher fracture energy of approximately 9000 J m^{-2} than those of pure SN forms of alginate and PAM gels which were approximately 25 and 150 J m^{-2}, respectively.[17]

To further improve the mechanical properties, the DN hydrogel was incorporated with many kinds of reinforcement, especially inorganic materials, for example, multiwalled carbon nanotubes (MWCNTs),[18] nanoclays (NC),[19] nanosilica (NS),[20] glass fibers,[21] and cellulose.[5,12,14,22] Among these, cellulose fiber (CF), a green material derived from plants, has drawn a lot of attention due to its low density, high surface area, good biocompatibility, and remarkable mechanical properties.[12,23,24] The comparative studies of three different

Received: April 9, 2022
Accepted: July 4, 2022
Published: July 13, 2022

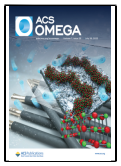

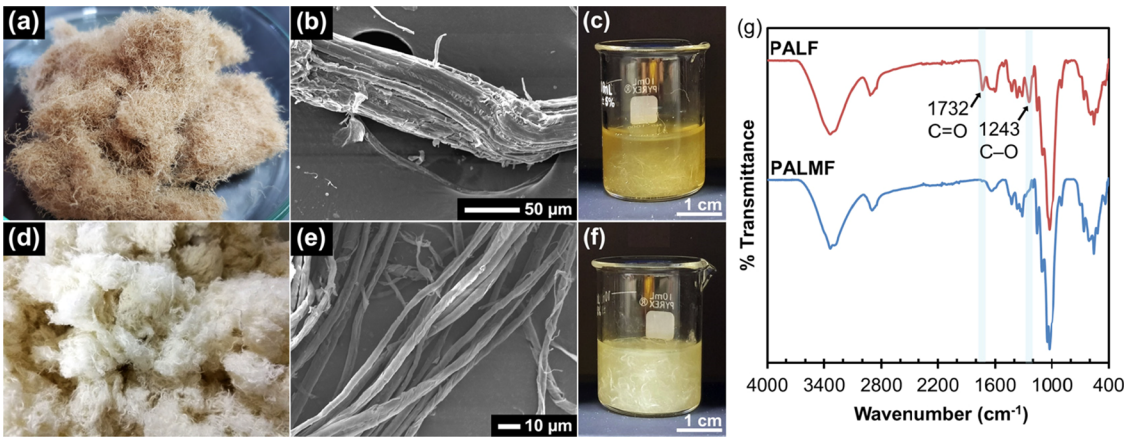

Figure 1. Photographs and SEM images of (a,b) PALF and (d,e) PALMF, (c) PALF and (f) PALMF dispersion in sodium alginate solution, and (g) ATR-FTIR spectra of fibers.

nanocelluloses, that is, cellulose nanocrystals (CNC), bacterial cellulose (BC) nanofibers, and 2,2,6,6-tetramethylpiperidine-1-oxy (TEMPO) radical-oxidized cellulose nanofibers (TOCN), as reinforcing fillers for DN hydrogels were reported.[14] It was found that BC with a high aspect ratio can strengthen the DN hydrogel almost 7 times higher than that of the neat one. Besides the aspect ratio, the mechanical properties of natural fibers mainly depend on the cellulose content and microfibrillar angle.[25] It was reported that the CF isolated from pineapple leaf (known as pineapple leaf fiber, PALF) contains a high cellulose content of 70−82% along with a very low microfibrillar angle of 5.6−14°.[25−27] PALF provides excellent mechanical properties including high tensile strength of 413−1627 MPa and Young's modulus of 60−82 GPa.[25,26] The high content of hydroxyl groups on the PALF surface originated from cellulose, a major component, as well as lignin and hemicellulose, minor constituents, could facilitate strong interaction between the polymer matrix and fibers. Thus, the enhancement of mechanical strength can be expected. In addition, Thailand is a top country cultivating pineapple with a planting area of roughly 240,000 acres. Consequently, there is an enormous pineapple leaf waste around 20,000−25,000 tons/acre after harvesting.[28]

The objective of this paper is to investigate the reinforcing efficiency of natural fibers on DN hydrogels. Sodium alginate and polyacrylamide were used to construct the DN hydrogel. Cellulose microfiber extracted from pineapple leaf was used as a green reinforcement fiber. The microfiber was obtained by the defibrillation of large PALF bundles into a micron-size constituent called as pineapple leaf microfiber (PALMF). This provides the fiber with a much greater aspect ratio and hence greater reinforcement. The effect of fiber content on the compressive behavior and other properties of the hydrogel was evaluated.

2. RESULTS AND DISCUSSION

2.1. Morphology of PALF and PALMF. Figure 1a,d shows the photographs of PALF before and after alkaline treatment combined with a mechanical force from a handheld blender. The color of PALF changes from light brown to almost white for the treated PALF, indicating the successful bleaching process in alkaline solution. The morphology of both untreated and treated PALF is displayed in the SEM images (Figure 1b,e). PALF is clearly a fiber bundle composed of a lot of elementary fibers with a rough surface. After the alkaline treatment combined with mechanical shear force, the bundles were totally defibrillated to elementary microfibers or PALMF. Also, the surface of PALMF is much smoother than that of PALF. As a consequence, the treatment with alkaline solution could bleach and remove impurities or cementing substances, that is, lignin and hemicellulose, that glue the elementary fibers together to form fiber bundles.[29,30] The average diameter of PALMF measured from the SEM images is about 3.04 ± 0.65 μm, whereas the fiber length is 6 mm, equal to that of PALF. Therefore, the aspect ratio (l/d) of PALMF is approximately 2000.

2.2. Chemical Composition of Fibers. The chemical composition of the fibers was examined with ATR-FTIR spectroscopy. As shown in Figure 1g, the strong peaks at wavenumbers of 1054 and 1030 cm^{-1} are due to the C−O stretching of aliphatic C−OH vibration and C−O−C stretching of cellulose constituents, respectively.[12,14,31] After alkaline treatment, the chemical composition of the fiber changed slightly. The peak at 1731 cm^{-1} belonging to C═O stretching dramatically decreased, whereas the peak at 1244 cm^{-1} assigned to C−O stretching totally disappeared. Both are the characteristic peaks of the acetyl groups of hemicellulose.[32,33] This result indicates that most of hemicellulose has been removed. Our group has confirmed the extracted material after alkaline treatment by precipitation with glacial acetic acid and examined by FTIR spectroscopy.[32] The spectrum displays the characteristic peaks at 1163 and 1042 cm^{-1}, attributed to the C−O−C vibration and C−O and C−C stretching or C−OH bending of hemicellulose (Xylan).[34] However, the treatment with alkaline solution could not entirely remove lignin. The characteristic peak of lignin at 1317 cm^{-1}[31] still appears in the PALMF spectrum. The remaining lignin on the fiber surface was further confirmed by X-ray photoelectron spectroscopy (XPS), as reported in a previous study.[30] The C/O ratio of PALMF was 0.50, close to that of lignin (0.33).[35,36]

The chemical compositions of PALF and PALMF are shown in Table 1. The major component of PALF is holocellulose (85.49%) with a large cellulose proportion of 57.19%. In agreement with ATR-FTIR results, hemicellulose is mostly extracted after alkaline treatment, resulting in the increase in the cellulose content. PALMF has higher cellulose and holocellulose percentages of 92.16 and 96.09%, respectively,

https://doi.org/10.1021/acsomega.2c02221
ACS Omega 2022, 7, 25321−25328

Table 1. Chemical Composition of PALF and PALMF

chemical constituent (%)	PALF	PALMF
acid-insoluble lignin	7.82	2.54
acid-soluble lignin	2.61	2.23
holocellulose	85.49	96.09
cellulose	57.19	92.16

and a smaller proportion of lignin (acid-insoluble and acid-soluble fractions of 2.54 and 2.23%, respectively).

2.3. Fiber Dispersion. For the fiber to be appropriate for hydrogel reinforcement, the fiber should remain well dispersed in the matrix over the course of hydrogel preparation. To check this, PALF and PALMF were separately suspended in sodium alginate solution to monitor the dispersion behavior and settling down of the fibers. After leaving for 1 h, PALF completely settled down to the bottom, as displayed in Figure 1c. Unlike PALF, the microfibers remained suspended in the solution and illustrated good dispersion (Figure 1f). It could be noticed that although the alginate solution was relatively viscous, it could not prevent the settling down of PALF. This fiber settlement might be due to the sinking of large bundles of PALF much faster than the microfibers. Moreover, according to the alkaline treatment that removed the cementing materials on the fiber surface, a large number of hydroxyl groups on the surface of PALMF allow the formation of hydrogen bonds between PALMF and alginate chains, resulting in good and stable fiber distribution. Thus, PALMF is more suitable to be used as a reinforcing material for the hydrogel system.

2.4. Network Formation of Hydrogels. The network formation of SA/PAM hydrogels incorporated with PALMF is described, as shown in Figure 2. The first network of polyacrylamide (PAM) was obtained during the thermally initiated free-radical polymerization of AM and MBA. The SA chains remain entangled with PALMF in the single network (SN) hydrogel. When the SN hydrogel was immersed in $CaCl_2$ solution, the second network of SA was formed through the ionic cross-link between the carboxylate (−COO−) groups and Ca^{2+} ions. PALMF remained well dispersed in the DN system and could interact with the polymer matrix *via* hydrogen bonds.

2.5. Morphology of Freeze-Dried Hydrogels. The morphology of freeze-dried PALMF-reinforced DN hydrogels is observed with a scanning electron microscope, and the images are shown in Figure 3a,b. All hydrogels illustrate the interconnected porous network with varying pore size. It seems that the hydrogels with higher fiber contents have smaller and more uniform sizes. SPMF-0.2 has large pore sizes ranging from 3 to 27 μm ($\bar{X}$ = 10.46 ± 4.92 μm), whereas SPMF-0.6 possesses smaller pore sizes ranging from 3 to 15 μm ($\bar{X}$ = 7.55 ± 2.67 μm). The reduction in the average pore size is probably due to PALMF behaving like a nucleating agent[37] during freezing in the freeze-drying process. The formation of ice occurs on the fiber surface through heterogeneous ice nucleation (HIN), followed by ice propagation.[38,39] The hydroxyl groups on the surface of PALMF facilitate ice nucleation via hydrogen bonds between the −OH groups and ice nucleus.[40] Consequently, SPMF-0.6 with a higher fiber content would have more ice nucleation, resulting in the hydrogel after the drying process exhibiting a smaller pore size than the others.

2.6. Chemical Composition of Hydrogels. Figure 3c displays the ATR-FTIR spectra of PALMF along with different freeze-dried hydrogels. SA shows strong peaks at 1600 and 1408 cm^{-1} ascribed to asymmetric and symmetric −COO− stretching, respectively.[14,41] For PAM, peaks at wavenumbers of 3333 and 3187 cm^{-1} are attributed to the symmetric vibration and asymmetric vibration of N−H, respectively.[41] The absorption bands located at 1649 and 1420 cm^{-1} are assigned to the C═O stretching and C−N stretching of $-CONH_2$, respectively.[14,41] The characteristic peaks of PALMF are interpreted in Section 2.2.

The spectra of SPMF hydrogels display broader bands ranging from 3000 to 3650 cm^{-1} attributed to the overlap between the −OH stretching of PALMF and SA and the N−H vibration of PAM. The absorption band located at 3193 cm^{-1} is responsible for the intermolecular N···H stretching between the N atom of PAM and H atom of SA.[14] The characteristic peak of C═O stretching is slightly shifted from 1649 to 1654 cm^{-1} owing to the intermolecular hydrogen bond between the two polymers.[42] Because of the large amount of fiber content, the strong peaks of cellulose at 1054 and 1029 cm^{-1} appear in the spectrum of SPMF-0.6. whereas SPMF-0.2 displays weaker bands. There is no other observable new absorption band in both the hydrogel spectra, indicating no new chemical bonds were formed between PAM, SA, and PALMF.

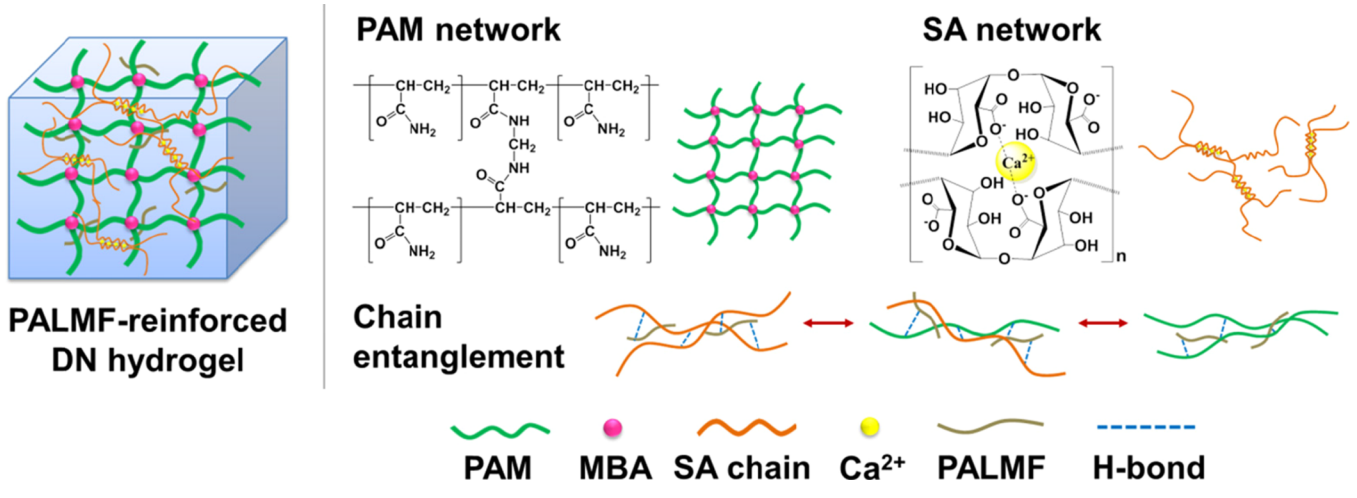

Figure 2. Schematic illustration of network formation in PALMF-reinforced DN hydrogels.

https://doi.org/10.1021/acsomega.2c02221
ACS Omega 2022, 7, 25321−25328

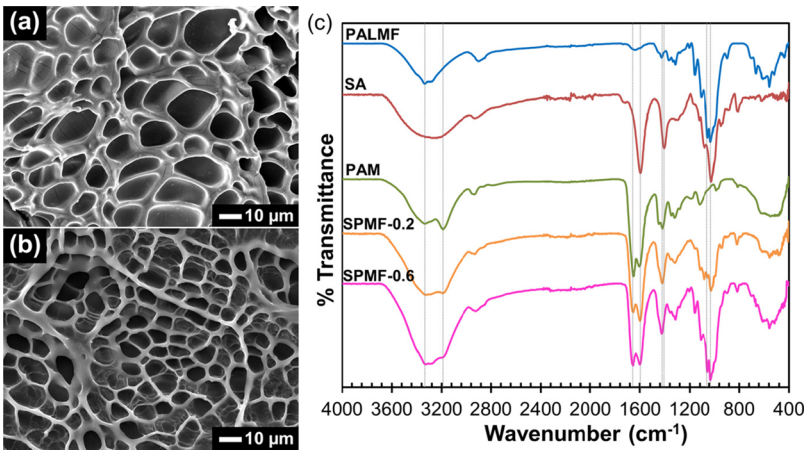

Figure 3. SEM images of freeze-dried DN hydrogels (a) SPMF-0.2 and (b) SPMF-0.6 and (c) ATR-FTIR spectra of PALMF, SA, PAM, and freeze-dried DN hydrogels.

2.7. Swelling Behavior. The swelling behavior of unreinforced and PALMF-reinforced SN and DN hydrogels was studied by immersing the hydrogels in deionized water for 100 h, and the results are shown in Figure 4. It is noticeable

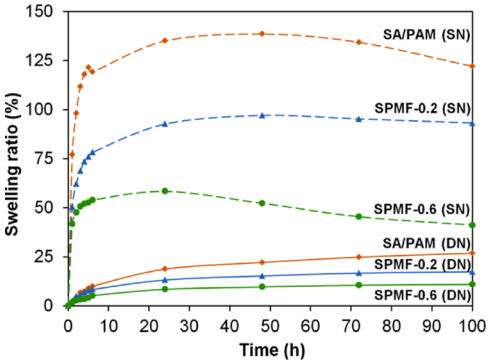

Figure 4. Swelling ratio of SN and DN hydrogels after immersion in water for 100 h.

that all SN hydrogels rapidly adsorb water, with high swelling rates in the initial stage. Then, the swelling rate decreases and reaches an equilibrium swelling ratio after soaking for 24 h or slightly drops at a longer immersion time. SN hydrogels containing PALMF demonstrate a lower swelling ratio, and the greater the amount of PALMF, the lower is the swelling ratio. The swelling ratio of SPMF-0.6 tends to decrease gradually and reaches a stable value at a longer immersion time. This is due to some weak bonds broken during excessive swelling, causing some small molecules leaving from the matrix.[43,44] DN hydrogels display similar swelling behavior to SN hydrogels but with a much lower swelling ratio. Unreinforced hydrogels (SA/PAM) show the highest water adsorption, followed by that reinforced with an increasing amount of PALMF. Unlike SN hydrogels, none of the DN hydrogels display a drop in the swelling ratio at long a immersion time.

Again, equilibrium swelling ratios (after 100 h) of SN hydrogels are much higher than that of DN hydrogels, and the swelling ratio decreases with the increasing fiber content. It is likely that the introduction of PALMF into the system provides additional hydrogen bonds between the fibers and the polymer matrix, leading to a greater cross-link density. In a similar manner, introducing a DN reduces the equilibrium swelling ratio. The equilibrium swelling ratio of the unreinforced hydrogel dropped from 122% for SN to 27% for DN, almost 5 times lower, and further decreased after being reinforced with fibers. An increasing number of junction points in PALMF-reinforced DN hydrogels could obstruct the diffusion of water molecules, resulting in the lower swelling degree.[3]

2.8. Gel Fraction. The gel contents of unreinforced and reinforced DN hydrogels were determined by immersing the gel in three different pH media. In responding to media pH, the functional groups of the hydrogel network could be protonated or deprotonated depending on the pKa value of that specific group.[41] As a result, hydrogen bonds (between different groups) and ionic bonds could either be weakened or strengthened.[27,41,45] When some bonds are weakened, parts of the network could be released into the solution, giving low gel fractions. It is found that gel fractions for the unreinforced system (SA/PAM) are very similar in all pH media, that is, 57.78, 57.78, and 58.08% for pH 3, DI water, and pH 10, respectively. There is a slight increasing trend with pH. The gel fraction for the PALMF-reinforced system (SPMF-0.6) is slightly higher than that of the unreinforced one. It is 58.13% in acid, 58.96% in DI water, and 59.02% in base.

2.9. Compression Property. The mechanical properties of unreinforced hydrogels and that reinforced with PALMF were determined using the compression test, and the results are shown separately for SN and DN systems in Figure 5. The

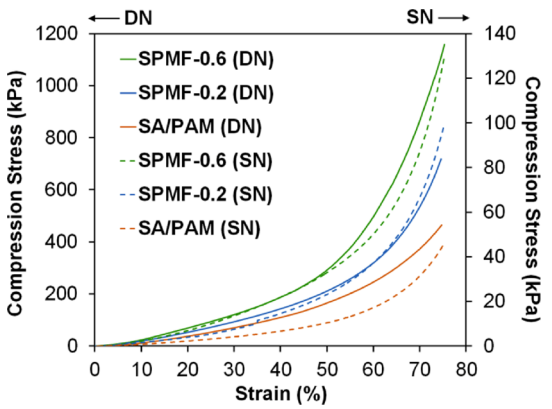

Figure 5. Stress−strain curves of SA/PAM and SPMF SN and DN hydrogels.

https://doi.org/10.1021/acsomega.2c02221
ACS Omega 2022, 7, 25321−25328

Table 2. Comparison of Hydrogels Prepared from the SA/PAM System Reinforced with Various Materials on Compression Property[a]

hydrogel system	reinforcement		length	diameter	60% strain		75% strain		ref
	source	wt %	(nm)	(nm)	stress (MPa)	% improv.	stress (MPa)	% improv.	
SA−PAM−CNC hydrogel	CNC extracted from bleached wood pulp fibers	0.1	176	10	0.44	52	∼2.50	150	14
oxidized CNC-reinforced oxidized alginate (Alg-CHO)/PAM hydrogel	oxidized CNC (CNC-CHO)	1.5	100	5	∼0.12	300	∼0.60	500	46
CNC-reinforced PAM/SA/silica glass hydrogel	CNC extracted from MCC	10	40−290	5−35	∼0.13	63			15
PALMF-reinforced SA/PAM hydrogel	PALMF	0.6	6 mm	∼3 μm	0.51	104	1.16	147	this work

[a]%Improv. = % Improvement of stress compared with that of pristine hydrogel without the addition of reinforcement.

SA/PAM SN hydrogel exhibits a stress of 46 kPa at 75% strain, and as the amount of PALMF increases, the stress increases. Stresses obtained at the highest compression strain of 75% for PALMF contents of 0.2 and 0.6 SN hydrogels are 99 and 130 kPa, respectively. It is obvious that the introduction of only 0.2 wt % reinforcing fiber can moderately improve the mechanical properties of the SN hydrogel. The hydroxyl groups on the surface of very stiff PALMF form hydrogen bonds with the polymer matrix, leading to the enhancement of physical cross-link density and subsequently leading to the higher hydrogel strength.[14]

Effect of introducing the second network and PALMF will now be considered. At a strain of 75%, the DN hydrogel displays a stress of 465 kPa, which is 10 times higher than that of the SN one, even though both contain SA inside the structure. This result suggests that the significant increase of compressive stress arose from the DN structure. Addition of PALMF into the DN system caused a similar increase in the stress, as seen in the SN system. At the strain of 75%, DN hydrogels with 0.2 and 0.6 wt % PALMF show compressive stresses of 718 and 1158 kPa, respectively. The effect of PALMF in the DN hydrogel is much stronger than that seen in the SN hydrogel, suggesting the synergistic effect of the second network and the reinforcing fiber.

Different cellulosic materials, especially cellulose nanocrystals (CNC), have been used to reinforce hydrogels, and their effectiveness will be compared with that of PALMF. The data are shown in Table 2. There are, however, contradicting evidences regarding the reinforcing effectiveness of CNC for hydrogels. The very high surface area of CNC could be expected to give very high reinforcement efficiency, and a small addition of only 0.1 wt % has been reported to improve the compressive stress significantly.[14] However, for hydrogels containing silica glass, the reinforcing efficiency of CNC appeared not so good. A very high loading of 10 wt % CNC provided a similar level of improvement, as 0.1 wt % in the previous case.[15] The possible reason for the low compressive stress is the high viscosity of the solution mixture containing silica sol−gel and $CaCl_2$, together with the inadequate reaction time, which could retard the mobility of certain molecules, subsequently resulting in the slow polymerization of AM and reduction in the cross-link density. As a consequence, the mechanical property is not as high as expected. For oxidized CNC, greater reinforcing efficiency could be anticipated, and this is shown by the work of Tang et al.[46] However, for a similar level of reinforcement with unmodified CNC, about 0.6 wt % of PALMF is required. This could be attributed to the very high aspect ratio of PALMF, which is about 2000 compared with that about 20−60 for CNC.[15,19,46]

It has been reported that although the DN structure can enhance the mechanical properties of hydrogels, it is still vulnerable to water swelling that could deteriorate the hydrogel strength.[47,48] In this study, this issue was alleviated by reinforcing the DN hydrogel with PALMF. According to the high cross-link density, the synthesized 0.6% PALMF-reinforced SA/PAM DN hydrogel reveals a small volume of water adsorption after soaking in water for 100 h. In other words, the DN hydrogel incorporated with PALMF provides a good swelling resistance in water. The introduction of PALMF into the DN hydrogel also strengthens the mechanical property with good compressive stress. Therefore, PALMF containing a high cellulose content and possessing a high aspect ratio can be used as a good reinforcing material for hydrogels. Furthermore, considering the convenience and energy required for the material preparation, PALMF provides a much more convenient route with much less energy required.[49]

3. CONCLUSIONS

PALMF-reinforced SN and DN SA/PAM hydrogels were prepared, and their mechanical behavior under compressive force was investigated. Both the network type and PALMF affect the mechanical behavior significantly. At the same level of compressive deformation, the stress required to deform the DN hydrogel is about 10 times (1000%) higher than that for the SN hydrogel. With the addition of less than 0.6% of PALMF, the corresponding stress increases further by about 3 times, indicating a synergistic effect of the microfiber and the second network. Other properties are also affected but with a much lower degree. This study provides an efficient method for preparing stiffer and stronger hydrogels which can be utilized in many applications.

4. EXPERIMENTAL SECTION

4.1. Materials. Ground pineapple leaf was prepared according to the previously described method[50] with slight modifications. Briefly, mature pineapple leaves were cut into small pieces of 6 mm in length across the leaf long axis. These were then ground using a motorized stone grinder, and the mash was dried under the sun. The ground materials were received from pineapple plantation in Ban Yang District, Phitsanulok, Thailand, and PALF was separated by simple sieving. Acrylamide monomer (AM, ≥98.0%), sodium alginate (SA, viscosity = 15−25 cP, 1% in H_2O), and ionic cross-linker calcium chloride ($CaCl_2$, anhydrous) were purchased from Sigma-Aldrich (China and United Kingdom). Potassium

https://doi.org/10.1021/acsomega.2c02221
ACS Omega 2022, 7, 25321−25328

persulfate (KPS, 97.0%) was obtained from Ajax Finechem (Australia). *N*,*N*′-methylenebisacrylamide (MBA, ≥98.0%) from Tokyo Chemical Industry Co., Ltd. (Japan) was used as a cross-linker. All chemicals were used without purification.

4.2. Preparation of PALMF. The preparation process of PALMF followed the method described by Surajarusarn et al.[30] In brief, 100 g of short PALF with the length of 6 mm was immersed in 3000 mL of NaOH solution (10% w/v) for 30 min. Then, the fiber suspension was treated with a handheld high-speed food blender (Buono, China) for 30 min to break down the fiber bundles into individual microfibers. The treated fibers were then filtered and washed with tap water several times until pH became 7, followed by drying in a hot air oven at 70 °C overnight. The dried and entangled fibers were loosened with a bladed high-speed beater, and this yielded very soft and fluffy PALMFs.

4.3. Synthesis of DN Hydrogel Incorporated with PALMF. A predetermined amount of PALMF (Table 3) was suspended in 5 mL of solution containing 0.78 g of AM monomer, 0.006 g of KPS initiator, and 0.003 g of MBA cross-linker. Then, 0.2 g of SA was gradually added into the suspension under vigorous stirring until a uniform mixture was obtained. The mixture was then poured into a silicone mold. Subsequently, this mold was placed in a hydrothermal reactor and heated at 100 °C for 3 h in a hot air oven to initiate the polymerization of acrylamide (AM). After heating, a network of polyacrylamide (PAM) was formed as a SN hydrogel. The unpolymerized AM was removed by washing with water. To get a DN hydrogel, the SN gel was immersed in 15 mL of 0.5 M $CaCl_2$ at room temperature for 12 h. The hydrogel was then rinsed with water to remove the excess amount of Ca^{2+} on the surface and blotted with a filter paper. The DN hydrogel containing PALMF was obtained, designated as SA/PAM/PALMF (or SPMF) hydrogel. The as-prepared hydrogel was stored in a refrigerator to avoid water evaporation and placed in ambient atmosphere until reaching room temperature before analysis.

Table 3. Compositions of the Precursors for the Synthesis of Hydrogels

sample	KPS (g)	AM (g)	MBA (g)	PALMF (g or %(w/v) against H_2O)	SA (g)	H_2O (mL)
SA/PAM	0.006	0.786	0.003	0	0.2	5
SPMF-0.2	0.006	0.786	0.003	0.010 (0.2 wt %)	0.2	5
SPMF-0.6	0.006	0.786	0.003	0.030 (0.6 wt %)	0.2	5

4.4. Characterizations. *4.4.1. Morphology.* The morphologies of fibers and hydrogels were observed with a scanning electron microscope (SEM, JSM-IT500, JEOL, Japan). Before examination, PALF and PALMF were dried in a hot air oven at 60 °C for 24 h to remove moisture. For hydrogels, the samples were freeze-dried for 24 h to remove water inside the structure. All samples were coated with platinum and mounted on an aluminum stub with a conductive carbon tape.

4.4.2. Chemical Composition. To analyze the chemical composition of PALF, PALMF, and hydrogels, an attenuated total reflectance Fourier transform infrared spectrophotometer (ATR-FTIR, Frontier, PerkinElmer) was used at room temperature over a range from 4000 to 400 cm^{-1}. All samples were absolutely dried before analysis. The moisture of the fibers was removed by drying in a hot air oven at 70 °C for 2 h, whereas freeze-drying technique was used to remove water inside hydrogels. Additionally, the chemical compositions in terms of acid-insoluble lignin, acid-soluble lignin, holocellulose, and cellulose in PALF and PALMF were determined using standard methods.[51−54]

4.4.3. Swelling Behavior. The swelling behavior of the hydrogel was evaluated by immersing the hydrogel in water for a designated time at ambient temperature. The excess water on the swollen hydrogel surface was blotted with a filter paper before measurement to obtain the exact weight. After weighing, the swollen hydrogel was put back in water again for further adsorption. The examination was conducted until reaching equilibrium. The swelling ratio was calculated using the following equation:

$$\text{Swelling ratio} = \frac{W_t - W_o}{W_o} \times 100$$

where W_o is the weight (g) of the sample before swelling, and W_t is the weight (g) of the swollen hydrogel after immersion in water at time t.

4.5. Gel Fraction. The freeze-dried hydrogels were immersed in three different mediums, namely, hydrochloric acid (pH 3), DI water (pH 5−6), and sodium hydroxide (pH 10) at ambient temperature for 4 days. After immersion, the hydrogels were freeze-dried again and re-weighed to estimate the hydrogel mass. The gel fraction was calculated using the following equation:

$$\text{Gel fraction} = \frac{W_f}{W_i} \times 100$$

where W_i and W_f are the weights (g) of the freeze-dried hydrogels before and after soaking in the medium, respectively.

4.6. Mechanical Property. Hydrogel specimens of cylindrical shape were prepared with diameters of approximately 23−25 mm and height of 7−10 mm, depending on the hydrogel type (SN or DN structure). The compression test was carried out using a universal testing machine (Instron Model 5566) with a 5 kN load cell. The measurement was performed with a constant crosshead rate of 5 mm min^{-1}. The compression stress (σ) was calculated using the following equation:

$$\sigma = \frac{F}{\pi r^2}$$

where F is the load force and r is the radius of the specimen. Compression strain (ε) is calculated according to the following equation:

$$\varepsilon = \frac{h_o - h}{h_o} \times 100\%$$

where h is the change in height, and h_o is the original height.

AUTHOR INFORMATION

Corresponding Author

Taweechai Amornsakchai − *Polymer Science and Technology Program, Department of Chemistry and Center of Excellence for Innovation in Chemistry, Faculty of Science and Center of Sustainable Energy and Green Materials, Faculty of Science, Mahidol University, Nakhon Pathom 73170, Thailand;*

https://doi.org/10.1021/acsomega.2c02221
ACS Omega 2022, 7, 25321−25328

orcid.org/0000-0002-5462-9192;
Email: taweechai.amo@mahidol.ac.th

Authors

Nithinan Sriraveeroj − *Polymer Science and Technology Program, Department of Chemistry and Center of Excellence for Innovation in Chemistry, Faculty of Science, Mahidol University, Nakhon Pathom 73170, Thailand*

Panya Sunintaboon − *Polymer Science and Technology Program, Department of Chemistry and Center of Excellence for Innovation in Chemistry, Faculty of Science, Mahidol University, Nakhon Pathom 73170, Thailand*

Anyarat Watthanaphanit − *Polymer Science and Technology Program, Department of Chemistry and Center of Excellence for Innovation in Chemistry, Faculty of Science, Mahidol University, Nakhon Pathom 73170, Thailand;* orcid.org/0000-0002-3649-7456

Complete contact information is available at: https://pubs.acs.org/10.1021/acsomega.2c02221

Notes

The authors declare no competing financial interest.

■ ACKNOWLEDGMENTS

The authors gratefully acknowledge the financial supports by Mahidol University (Basic Research Fund: fiscal year 2022). The authors also acknowledge the scholarship from the Science Achievement Scholarship of Thailand (SAST) provided for NS. The authors thank Mahidol University Frontier Research Facility (MU-FRF) for instrument support and the MU-FRF scientists, Nawapol Udpuay, Chawalit Takoon, and Dr. Suwilai Chaveanghong, for their kind assistance in the operation of SEM.

■ REFERENCES

(1) Bahrami, Z.; Akbari, A.; Eftekhari-Sis, B. Double network hydrogel of sodium alginate/polyacrylamide cross-linked with POSS: Swelling, dye removal and mechanical properties. *Int. J. Biol. Macromol.* **2019**, *129*, 187−197.

(2) Sakai, T.; Matsunaga, T.; Yamamoto, Y.; Ito, C.; Yoshida, R.; Suzuki, S.; Sasaki, N.; Shibayama, M.; Chung, U.-I. Design and fabrication of a high-strength hydrogel with ideally homogeneous network structure from tetrahedron-like macromonomers. *Macromolecules* **2008**, *41*, 5379−5384.

(3) Sheng, C.; Zhou, Y.; Zhang, X.; Xue, G. Mechanical, thermal, and swelling properties of cross-linked hydrogels based on oxidized cellulose nanowhiskers and chitosan/poly(vinyl alcohol) blends. *Fibers Polym.* **2018**, *19*, 2030−2038.

(4) Ma, X.; Xu, T.; Chen, W.; Wang, R.; Xu, Z.; Ye, Z.; Chi, B. Improvement of toughness for the hyaluronic acid and adipic acid dihydrazide hydrogel by PEG. *Fibers Polym.* **2017**, *18*, 817−824.

(5) Bai, C.; Huang, X.; Xie, F.; Xiong, X. Microcrystalline cellulose surface-modified with acrylamide for reinforcement of hydrogels. *ACS Sustainable Chem. Eng.* **2018**, *6*, 12320−12327.

(6) Okumura, Y.; Ito, K. The polyrotaxane gel: A topological gel by figure-of-eight cross-links. *Adv. Mater.* **2001**, *13*, 485−487.

(7) Ishii, S.; Kokubo, H.; Hashimoto, K.; Imaizumi, S.; Watanabe, M. Tetra-PEG network containing ionic liquid synthesized via michael addition reaction and its application to polymer actuator. *Macromolecules* **2017**, *50*, 2906−2915.

(8) Gong, J. P.; Katsuyama, Y.; Kurokawa, T.; Osada, Y. Double-network hydrogels with extremely high mechanical strength. *Adv. Mater.* **2003**, *15*, 1155−1158.

(9) Ma, J.; Zhou, G.; Chu, L.; Liu, Y.; Liu, C.; Luo, S.; Wei, Y. Efficient removal of heavy metal ions with an EDTA functionalized chitosan/polyacrylamide double network hydrogel. *ACS Sustainable Chem. Eng.* **2017**, *5*, 843−851.

(10) Shibayama, M.; Karino, T.; Miyazaki, S.; Okabe, S.; Takehisa, T.; Haraguchi, K. Small-angle neutron scattering study on uniaxially stretched poly(N-isopropylacrylamide)−clay nanocomposite gels. *Macromolecules* **2005**, *38*, 10772−10781.

(11) Moniruzzaman, M.; Winey, K. I. Polymer nanocomposites containing carbon nanotubes. *Macromolecules* **2006**, *39*, 5194−5205.

(12) Yang, X.; Wang, L.; Yano, H.; Abe, K. Toughened hydrogels through UV grafting of cellulose nanofibers. *ACS Sustainable Chem. Eng.* **2021**, *9*, 1507−1511.

(13) Liu, S.; Zhong, Y.; Zhang, X.; Pi, M.; Wang, X.; Zhu, R.; Cui, W.; Ran, R. Highly Deformable, Conductive Double-Network Hydrogel Electrolytes for Durable and Flexible Supercapacitors. *ACS Appl. Mater. Interfaces* **2022**, *14*, 15641−15652.

(14) Yue, Y.; Wang, X.; Han, J.; Yu, L.; Chen, J.; Wu, Q.; Jiang, J. Effects of nanocellulose on sodium alginate/polyacrylamide hydrogel: Mechanical properties and adsorption-desorption capacities. *Carbohydr. Polym.* **2019**, *206*, 289−301.

(15) Kumar, A.; Rao, K. M.; Han, S. S. Synthesis of mechanically stiff and bioactive hybrid hydrogels for bone tissue engineering applications. *Chem. Eng. J.* **2017**, *317*, 119−131.

(16) Zhao, D.; Wang, X.; Cheng, B.; Yin, M.; Hou, Z.; Li, X.; Liu, K.; Tie, C.; Yin, M. Degradation-Kinetics-Controllable and Tissue-Regeneration-Matchable Photocross-linked Alginate Hydrogels for Bone Repair. *ACS Appl. Mater. Interfaces* **2022**, *14*, 21886.

(17) Darnell, M. C.; Sun, J. Y.; Mehta, M.; Johnson, C.; Arany, P. R.; Suo, Z.; Mooney, D. J. Performance and biocompatibility of extremely tough alginate/polyacrylamide hydrogels. *Biomaterials* **2013**, *34*, 8042−8048.

(18) Thibodeau, J.; Ignaszak, A. Flexible electrode based on MWCNT embedded in a cross-linked acrylamide/alginate blend: Conductivity vs. Stretching. *Polymers* **2020**, *12*, 181.

(19) Yue, Y.; Wang, X.; Wu, Q.; Han, J.; Jiang, J. Assembly of polyacrylamide-sodium alginate-based organic-inorganic hydrogel with mechanical and adsorption properties. *Polymer* **2019**, *11*, 1239.

(20) Arjmandi, M.; Ramezani, M. Mechanical and tribological assessment of silica nanoparticle-alginate-polyacrylamide nanocomposite hydrogels as a cartilage replacement. *J. Mech. Behav. Biomed. Mater.* **2019**, *95*, 196−204.

(21) Martin, N.; Youssef, G. Dynamic properties of hydrogels and fiber-reinforced hydrogels. *J. Mech. Behav. Biomed. Mater.* **2018**, *85*, 194−200.

(22) Nguyen, V. T.; Ha, L. Q.; Nguyen, T. D. L.; Ly, P. H.; Nguyen, D. M.; Hoang, D. Nanocellulose and Graphene Oxide Aerogels for Adsorption and Removal Methylene Blue from an Aqueous Environment. *ACS Omega* **2022**, *7*, 1003−1013.

(23) Freitas, P. A. V.; Arias, C. I. L. F.; Torres-Giner, S.; González-Martínez, C.; Chiralt, A. Valorization of rice straw into cellulose microfibers for the reinforcement of thermoplastic corn starch films. *Appl. Sci.* **2021**, *11*, 8433.

(24) Pinkas, O.; Haneman, O.; Chemke, O.; Zilberman, M. Fiber-reinforced composite hydrogels for bioadhesive and sealant applications. *Polym. Adv. Technol.* **2017**, *28*, 1162−1169.

(25) Radoor, S.; Karayil, J.; Sanjay, M. R.; Siengchin, S.; Parameswaranpillai, J. A review on the extraction of pineapple, sisal and abaca fibers and their use as reinforcement in polymer matrix. *eXPRESS Polym. Lett.* **2020**, *14*, 309−335.

(26) Asim, M.; Abdan, K.; Jawaid, M.; Nasir, M.; Dashtizadeh, Z.; Ishak, M. R.; Hoque, M. E. A review on pineapple leaves fibre and its composites. *Int. J. Polym. Sci.* **2015**, *2015*, No. 950567.

(27) Noipitak, P.; Inphonlek, S.; Nillawong, M.; Sunintaboon, P.; Amornsakchai, T. Chitosan/alginate composite porous hydrogels reinforced with PHEMA/PEI core−shell particles and pineapple-leaf cellulose fibers: their physico-mechanical properties and ability to incorporate AgNP. *J. Polym. Res.* **2021**, *28*, 182.

(28) Kengkhetkit, N.; Amornsakchai, T. A new approach to "Greening" plastic composites using pineapple leaf waste for performance and cost effectiveness. *Mater. Des.* **2014**, *55*, 292−299.

(29) Kalia, S.; Kaith, B. S.; Kaur, I. Pretreatments of natural fibers and their application as reinforcing material in polymer composites—A review. *Polym. Eng. Sci.* **2009**, *49*, 1253−1272.
(30) Surajarusarn, B.; Hajjar-Garreau, S.; Schrodj, G.; Mougin, K.; Amornsakchai, T. Comparative study of pineapple leaf microfiber and aramid fiber reinforced natural rubbers using dynamic mechanical analysis. *Polym. Test.* **2020**, *82*, No. 106289.
(31) Hazarika, D.; Gogoi, N.; Jose, S.; Das, R.; Basu, G. Exploration of future prospects of Indian pineapple leaf, an agro waste for textile application. *J. Cleaner Prod.* **2017**, *141*, 580−586.
(32) Surajarusarn, B.; Traiperm, P.; Amornsakcha, T. Revisiting the morphology, microstructure, and properties of cellulose fiber from pineapple leaf so as to expand its utilization. *Sains Malays.* **2019**, *48*, 145−154.
(33) Sarah, S.; Rahman, W. A. W. A.; Majid, R. A.; Yahya, W. J.; Adrus, N.; Hasannuddin, A. K.; Low, J. H. Optimization of pineapple leaf fibre extraction methods and their biodegradabilities for soil cover application. *J. Polym. Environ.* **2018**, *26*, 319−329.
(34) Xiao, B.; Sun, X. F.; Sun, R. Chemical, structural, and thermal characterizations of alkali-soluble lignins and hemicelluloses, and cellulose from maize stems, rye straw, and rice straw. *Polym. Degrad. Stab.* **2001**, *74*, 307−319.
(35) Johansson, L.-S.; Campbell, J. M.; Koljonen, K.; Stenius, P. Evaluation of surface lignin on cellulose fibers with XPS. *Appl. Surf. Sci.* **1999**, *144−145*, 92−95.
(36) Tran, L. Q. N.; Fuentes, C. A.; Dupont-Gillain, C.; Van Vuure, A. W.; Verpoest, I. Wetting analysis and surface characterisation of coir fibres used as reinforcement for composites. *Colloids Surf., A* **2011**, *377*, 251−260.
(37) Septevani, A. A.; Evans, D. A. C.; Annamalai, P. K.; Martin, D. J. The use of cellulose nanocrystals to enhance the thermal insulation properties and sustainability of rigid polyurethane foam. *Ind. Crop. Prod.* **2017**, *107*, 114−121.
(38) Zhou, X.; Sun, Y.; Liu, J. Designing Anti-Icing Surfaces by Controlling Ice Formation. *Adv. Mater. Interfaces* **2021**, *8*, No. 2100327.
(39) Guo, Q.; He, Z.; Jin, Y.; Zhang, S.; Wu, S.; Bai, G.; Xue, H.; Liu, Z.; Jin, S.; Zhao, L.; Wang, J. Tuning Ice Nucleation and Propagation with Counterions on Multilayer Hydrogels. *Langmuir* **2018**, *34*, 11986−11991.
(40) Xue, H.; Lu, Y.; Geng, H.; Dong, B.; Wu, S.; Fan, Q.; Zhang, Z.; Li, X.; Zhou, X.; Wang, J. Hydroxyl Groups on the Graphene Surfaces Facilitate Ice Nucleation. *J. Phys. Chem. Lett.* **2019**, *10*, 2458−2462.
(41) Zheng, Q.; Zhao, L.; Wang, J.; Wang, S.; Liu, Y.; Liu, X. High-strength and high-toughness sodium alginate/polyacrylamide double physically crosslinked network hydrogel with superior self-healing and self-recovery properties prepared by a one-pot method. *Colloids Surf., A* **2020**, *589*, No. 124402.
(42) Zhao, D.; Feng, M.; Zhang, L.; He, B.; Chen, X.; Sun, J. Facile synthesis of self-healing and layered sodium alginate/polyacrylamide hydrogel promoted by dynamic hydrogen bond. *Carbohydr. Polym.* **2021**, *256*, No. 117580.
(43) Zareie, C.; Sefti, M. V.; Bahramian, A. R.; Salehi, M. B. A polyacrylamide hydrogel for application at high temperature and salinity tolerance in temporary well plugging. *Iran. Polym. J.* **2018**, *27*, 577−587.
(44) Zareie, C.; Bahramian, A. R.; Sefti, M. V.; Salehi, M. B. Network-gel strength relationship and performance improvement of polyacrylamide hydrogel using nano-silica; with regards to application in oil wells conditions. *J. Mol. Liq.* **2019**, *278*, 512−520.
(45) Zhang, H.; Pang, X.; Qi, Y. pH-Sensitive graphene oxide/sodium alginate/polyacrylamide nanocomposite semi-IPN hydrogel with improved mechanical strength. *RSC Adv.* **2015**, *5*, 89083−89091.
(46) Tang, J.; Javaid, M. U.; Pan, C.; Yu, G.; Berry, R. M.; Tam, K. C. Self-healing stimuli-responsive cellulose nanocrystal hydrogels. *Carbohydr. Polym.* **2020**, *229*, No. 115486.
(47) Fan, H.; Wang, J.; Jin, Z. Tough, swelling-resistant, self-healing, and adhesive dual-cross-linked hydrogels based on polymer−tannic acid multiple hydrogen bonds. *Macromolecules* **2018**, *51*, 1696−1705.
(48) Kamata, H.; Akagi, Y.; Kayasuga-Kariya, Y.; Chung, U.-I.; Sakai, T. "Nonswellable" hydrogel without mechanical hysteresis. *Science* **2014**, *343*, 873−875.
(49) Joshi, S. V.; Drzal, L. T.; Mohanty, A. K.; Arora, S. Are natural fiber composites environmentally superior to glass fiber reinforced composites? *Composites, Part A* **2004**, *35*, 371−376.
(50) Kengkhetkit, N.; Amornsakchai, T. Utilisation of pineapple leaf waste for plastic reinforcement: 1. A novel extraction method for short pineapple leaf fiber. *Ind. Crop. Prod.* **2012**, *40*, 55−61.
(51) Wise, L. E.; Murphy, M.; Adieco, A. A. D. A chlorite holocellulose, its fractionation and bearing on summative wood analysis and studies on the hemicelluloses. *Pap. Trade J.* **1946**, *122*, 35−43.
(52) Updegraff, D. M. Semimicro determination of cellulose inbiological materials. *Anal. Biochem.* **1969**, *32*, 420−424.
(53) TAPPI, TAPPI T-222-om-21. In *Acid-insoluble lignin in wood and pulp*; 2007.
(54) TAPPI, TAPPI T-UM 250. In *Acid-Soluble Lignin in Wood and Pulp*; 2007.

https://doi.org/10.1021/acsomega.2c02221
ACS Omega 2022, 7, 25321−25328